Bull. Mater. Sci., Vol. 36, No. 5, October 2013, pp. 813–818. © Indian Academy of Sciences.

Swift heavy ion irradiation induced modification of structure and surface morphology of $BiFeO_3$ thin film

B N DASH[1,3,*], P MALLICK[2,3], P DASH[3], R BISWAL[3], JAI PRAKASH[4], A TRIPATHI[4], D KANJILAL[4] and N C MISHRA[3]

[1]Department of Physics, Salipur College, Salipur 754 103, India
[2]Department of Physics, North Orissa University, Baripada 757 003, India
[3]Department of Physics, Utkal University, Bhubaneswar 751 004, India
[4]Inter-University Acceleration Centre, Aruna Asaf Ali Marg, New Delhi 110 067, India

MS received 15 March 2012; revised 3 May 2012

Abstract. **$BiFeO_3$ (BFO) thin films of thickness about 800 nm deposited on Si (100) substrates by sol–gel spin coating method were irradiated by 200 MeV Ag ions. Modification of structure and surface morphology of the films under irradiation was studied using glancing incidence X-ray diffraction (GIXRD) and atomic force microscope (AFM). Fluence dependence of GIXRD peak intensity indicated formation of 10 nm diameter cylindrical amorphous columns in crystalline BFO due to 200 MeV Ag ion irradiation. AFM analysis indicated that the pristine film consists of agglomerated grains with diffuse grain boundary. Irradiation led to reduced agglomeration of the grains with the formation of sharper grain boundaries. The rms roughness (σ_{rms}) estimated from AFM analysis increased from 6·2 in pristine film to 12·7 nm when the film irradiated at a fluence of 1×10^{11} ions cm^{-2}. Further irradiation led to decrease of σ_{rms} which finally saturated at a value of 7–8 nm at high ion fluences. The power spectral density analysis indicated that the evolution of surface morphology of the pristine film is governed by the combined effect of evaporation condensation and volume diffusion processes. Swift heavy ion irradiation seems to increase the dominance of volume diffusion in controlling surface morphology of the film at high ion fluences.**

Keywords. **Ion irradiation; nanoparticles; atomic force microscopy; $BiFeO_3$.**

1. Introduction

Materials that simultaneously exhibit electric and magnetic ordering with an intimate coupling of both the ordered states have attracted considerable attention due to their promising multifunctional device applications. In recent years, $BiFeO_3$ (BFO) has been extensively studied due to the existence of both magnetic and strong ferroelectric order at room temperature (Catalan and Scott 2009). BFO shows ferroelectric ordering below ferroelectric Curie temperature (T_C) of ~1100 K and also shows G-type antiferromagnetic order below antiferromagnetic Nèel temperature (T_N) of ~640 K (Wang *et al* 2004). It has rhombohedrally distorted perovskite structure with space group $R3c$ (Michel *et al* 1969). The unit cell parameters are $a = 0{\cdot}396$ nm and $\alpha = 89°\ 28'$ (Blaauw and van der Woude 1973). Besides the robust multiferroic properties, BFO has been considered as a potential candidate for enhancement of piezoelectric coefficients with doping (Fujino *et al* 2008; Cheng *et al* 2010; Li *et al* 2011), data-storage media (Fiebig *et al* 2002), multiple-state memories (Hill 2000), terahertz emission source (Takahashi *et al* 2006), sensors (Michel *et al* 1969), magnetoelectric and spintronic applications (Bea *et al* 2008), etc. Many of these applications require BFO in thin film form and surface of the films plays a significant role in tailoring their suitability for specific applications.

BFO thin films have been fabricated by various physical parameters such as sputtering (Li *et al* 2008), pulsed laser deposition (Bark *et al* 2007), molecular beam epitaxy (Ihlefeld *et al* 2008), etc and chemical parameters such as metal–organic chemical vapour deposition (Yang *et al* 2005), sol–gel (Lee and Kim 2006), spray pyrolysis (Siwach *et al* 2007), etc methods. Several reports are available on the modification of microstructure and surface morphology of BFO thin films under different processing conditions such as thermal annealing (Lee and Kim 2006), annealing atmosphere (air or oxygen) (Iakovlev *et al* 2005; Siwach *et al* 2007), rapid thermal annealing (Naganuma and Okamura 2007), doping (Kim *et al* 2006), using excess Fe or Bi precursor (Kartavtseva *et al* 2007), substrate (Li *et al* 2005), etc. Irradiation by swift heavy ion has been considered as a unique post deposition processing technique for materials modification due to instantaneous (10^{-15}–10^{-12} s) energy deposition in highly localized region of few nm diameter. In addition to modifying the bulk, SHI irradiation has been shown to modify the surface morphology of thin film in a variety of systems (Sahasrabudhe *et al* 2007; Agarwal *et al* 2008; Kumar *et al* 2008; Mallick *et al* 2009, 2010; Kumaravel *et al* 2011).

*Author for correspondence (bichidash@yahoo.co.in)

In the present study, we report evolution of surface morphology of BFO films under 200 MeV Ag ion irradiation. Our study indicates that the evolution of surface morphology in pristine film is governed by the combined effect of evaporation–condensation and volume diffusion processes and ion irradiation shifts the mechanism of surface evolution towards volume diffusion.

2. Experimental

$BiFeO_3$ thin films were prepared on Si(100) substrate by sol–gel spin coating process (Liu *et al* 2006) using bismuth nitrate [$Bi(NO_3)_3{\cdot}5H_2O$] (Merck) and iron nitrate [$Fe(NO_3)_3{\cdot}9H_2O$] (Merck) as starting materials. Bismuth nitrate and iron nitrate were mixed with a molar ratio of 1:1 and dissolved at room temperature in 2-methoxyethanol and stirred for 30 min. Then acetic anhydride was added to dehydrate and ethanolamine was added to adjust the viscosity under constant stirring. The concentration of the stock solution was adjusted to 0·3 M by adding 2-methoxyethanol. The above process was performed in an ambient atmosphere at room temperature. Before spin coating, the substrates were cleaned by ultrasonication in alcohol and acetone. The depositions were carried out using Apex Instruments make spin coater (Model-SCU 2004) at 5500 rpm for 15 s. Each layer after deposition was annealed at 350 °C for 3 min in a tubular furnace. The spin coating and annealing were repeated 10 times to obtain BFO films of adequate thickness. In order to get the perovskite phase, films were annealed at 550 °C for 1 h.

The films were irradiated at 300 K with 200 MeV Ag ions using 16 MV tandem pelletron accelerator at IUAC, New Delhi. Maximum fluence used in the present study was 1×10^{13} ions cm^{-2}. Films fixed to the target ladder were placed inside the high vacuum ($\sim 10^{-6}$ torr) chamber during irradiation. Irradiation was performed in the direction nearly perpendicular to the sample surface. The ion beam was magnetically scanned over 1×1 cm^2 area covering the complete sample surface for uniform irradiation. Glancing angle X-ray diffraction (GAXRD) at room temperature with CuKα radiation using Bruker X-ray diffractometer (Model D8 Advanced) confirmed formation of BFO phase. Thickness of BFO thin film was found to be ~800 nm by using Rutherford backscattering spectrometry (RBS) technique. Evolution of surface morphology with ion fluence was investigated using atomic force microscope (AFM) (Digital instruments, Nanoscope IIIa).

3. Results and discussion

The electronic energy loss (S_e), nuclear energy loss (S_n) and range of 200 MeV Ag ion in BFO as estimated from SRIM-2010 simulation program are ~26 keV nm^{-1}, 0·08 keV nm^{-1} and 12 μm, respectively. Since the thickness of BFO films was much smaller than the range of the ion beam in BFO, energy deposition in the film is uniform. The large projectile range means that the ions are implanted much deeper in the substrate and S_n effect is negligible in the films. The observed modification in BFO matrix is, therefore, mainly due to S_e induced processes.

Figure 1 shows XRD pattern of pristine and 200 MeV Ag ion irradiated BFO films. BFO crystallizes in several phases, viz. rhombohedral, orthorhombic and tetragonal. XRD analysis indicates that the pristine BFO thin films used in the present study crystallized in rhombohedral phase and the films progressively amorphized with increasing ion fluence. Three new peaks at $2\theta = 21{\cdot}4$, 26·6 and 39·4 (* marked) appeared at the fluence of 1×10^{11} ions cm^{-2} and persisted up to the fluence of 3×10^{11} ions cm^{-2}. These peaks disappeared at higher fluences, whereas peaks due to the parent $BiFeO_3$ persisted up to the fluence of 1×10^{12} ions cm^{-2}. At still higher fluences the films got completely amorphized and all XRD peaks vanished.

Appearance of new peaks at intermediate fluences (1×10^{11} and 3×10^{11} ions cm^{-2}) indicate formation of some impurity phases induced by ion irradiation at these fluences. A comparison of these peaks with those reported in JCPDS file [card no. 71-2494] indicated that the impurity phase is $Bi_2Fe_4O_9$. It has been reported that $BiFeO_3$ is very unstable at high temperature and it rapidly decomposes into parasitic phases like $Bi_2Fe_4O_9$ or Fe_2O_3 (Catalan and Scott 2009). The formation of $Bi_2Fe_4O_9$ phase in our case may be due to the effect of increased temperature in the materials medium during the passage of 200 MeV Ag ions. This result, thus, supports the applicability of thermal spike model of ion-matter interaction in our case. Vanishing of these impurity peaks at higher fluences may be due to overlapping of the ion tracks leading to amorphization of these phases.

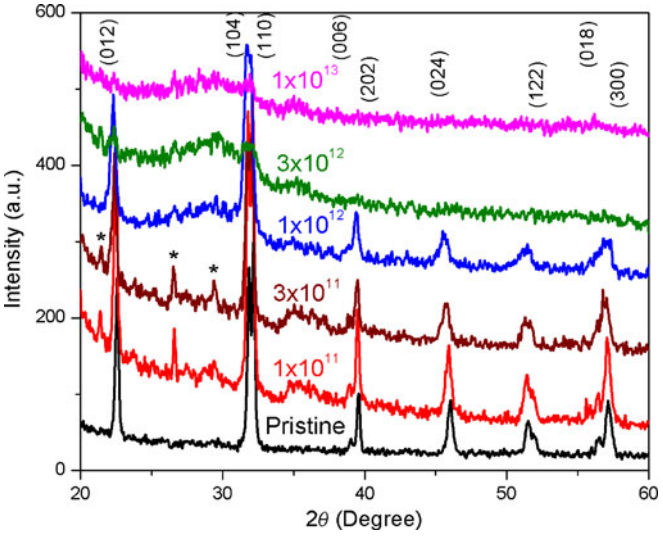

Figure 1. Evolution of XRD pattern with 200 MeV Ag ion irradiation fluence for $BiFeO_3$ thin films grown on Si(100) substrate. Impurity peaks corresponding to $Bi_2Fe_4O_9$ (* marked) appeared in intermediate ion fluences (1×10^{11} and 3×10^{11} ions cm^{-2}).

Since S_e of 200 MeV Ag ions in bulk BFO is comparable to its S_{eth} (~25 keV nm^{-1} (Studer *et al* 1997)), these ions can create extensive disorder along their path and hence, suppress the crystalline volume fraction with increasing ion fluence. Figure 2 shows variation of XRD peak intensity of [110] major peak of BFO as a function of ion fluence. The other peaks also show similar variation with ion fluence. The exponential decrease of XRD peak intensity indicated the formation of ion tracks of highly damaged cylindrical volumes that do not contribute to XRD crystallographic reflections. We, therefore, estimated the radius of ion track by fitting XRD intensity with ion fluence, $I(\phi)$, as per the following equation (Mallick *et al* 2012):

$$I(\phi) = a + be^{-A\Phi}, \tag{1}$$

where ϕ is the irradiation fluence, $A(=\pi r^2)$ the damage cross-section of a single ion track of radius 'r' and a and b are constants. The diameter of the ion track was estimated by fitting XRD intensity vs ion fluence to (1). The diameter was found to be 10 ± 2 nm. Complete amorphization is seen to occur at and above the fluence of 3×10^{12} ions cm^{-2}. At this fluence ion tracks are expected to overlap and the amorphization is a consequence of track overlap.

Figure 3 shows 2×2 μm two-dimensional (2-D) AFM images of the pristine film and the films irradiated with 200 MeV Ag ions at different fluences. The pristine film consists of agglomerated grains with diffuse grain boundary (figure 3(a)). Irradiation led to reduced agglomeration of the grains with sharper grain boundaries at all ion fluences except at the highest ion fluence (1×10^{13} ions cm^{-2}). Though sharp grain boundary could be seen at this fluence, each grain consisted of agglomeration of smaller grains. Figure 4 gives size distribution of the grains extracted from figure 3. The average value of grain size estimated from size distribution curve for different ion fluences is given in table 1. The size distribution of the grains for the pristine film and the film irradiated at the highest ion fluence could not be determined due to the problem of grain agglomeration (figures 3(a and f)).

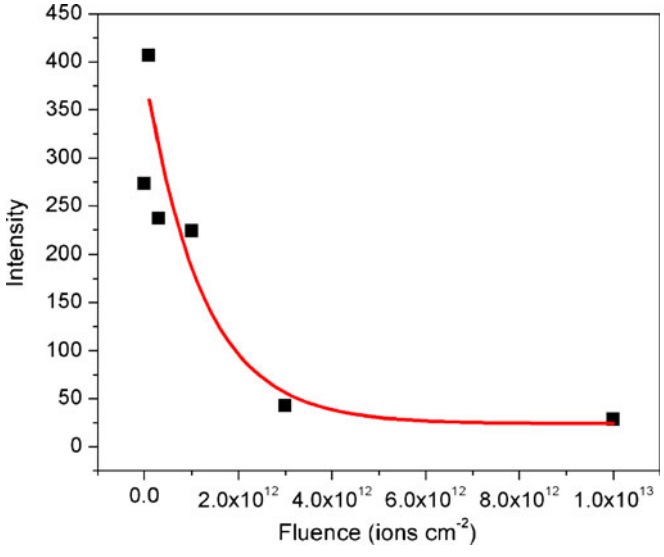

Figure 2. Variation of intensity of [110] XRD peak of BFO with ion fluence. Line represents fitting of data points to Poisson equation (1) yielding ion track diameter of 10 nm. Other peaks also show similar variation with ion fluence.

The surface morphology of BFO thin films, quantified in terms of the root mean square surface roughness, σ_{rms}, increased from 6·2 nm in pristine film to 12·7 nm in the film irradiated at a fluence of 1×10^{11} ions cm^{-2}. Further irradiation led to decrease of σ_{rms} which finally saturated at a value of ~7–8 nm at high ion fluence (table 1). The increased roughness at low fluence may be due to surface corrugation created by random heating of ions and the same reduced at high fluences due to the overlap of ion tracks leading to volume diffusion as discussed later.

In order to get quantitative information about the evolution of surface roughness along both vertical and lateral directions and to understand their possible origin, a study on power spectral density (PSD) is undertaken. Figure 5 shows evolution of PSD as a function of spatial frequency, q, for pristine and 200 MeV Ag ion irradiated BFO films in a log–log plot. The power spectra as shown in figure 5 can be divided into two distinct regions: (i) the low frequency region resembles the uncorrelated white noise and (ii) the straight line high frequency region represents correlated surface features. The surface corrugation defined as the slope of a line connecting two points on the surface, becomes small for points separated by a length longer than the correlation length, ξ_0 ($\xi_0 = 1/q_0$), where q_0 is the value of crossover wavevector. Thus, PSD function is expected to be independent of q for $q < q_0$. For length smaller than ξ_0 corresponding to high frequency region, corrugations become significant and PSD function of AFM images shows power-law dependence as (Eklund *et al* 1993):

$$\text{PSD} = Cq^{-\delta}, \tag{2}$$

where C is a constant and q the spatial frequency. The values of power-law exponent (δ) represent different modes of surface transport. From a simple linear dimensional analysis (Herring 1950), δ values of 1, 2, 3 and 4 have been shown to represent four modes of surface transport viz. viscous flow, evaporation–condensation, volume diffusion and surface diffusion, respectively. The estimated values of δ, obtained by fitting the experimental data using (2) to the high frequency region are given in table 1. The value of δ being 2·59 (lies between 2 and 3) for the pristine film indicated that the surface morphology in this case is due to the combined effect of evaporation–condensation and volume diffusion with almost equal contribution of both the processes. Irradiation by 200 MeV Ag ions led to an increase of δ from 2·59 to a value close to 3 at different ion fluences indicating the dominance of volume diffusion processes. δ is further

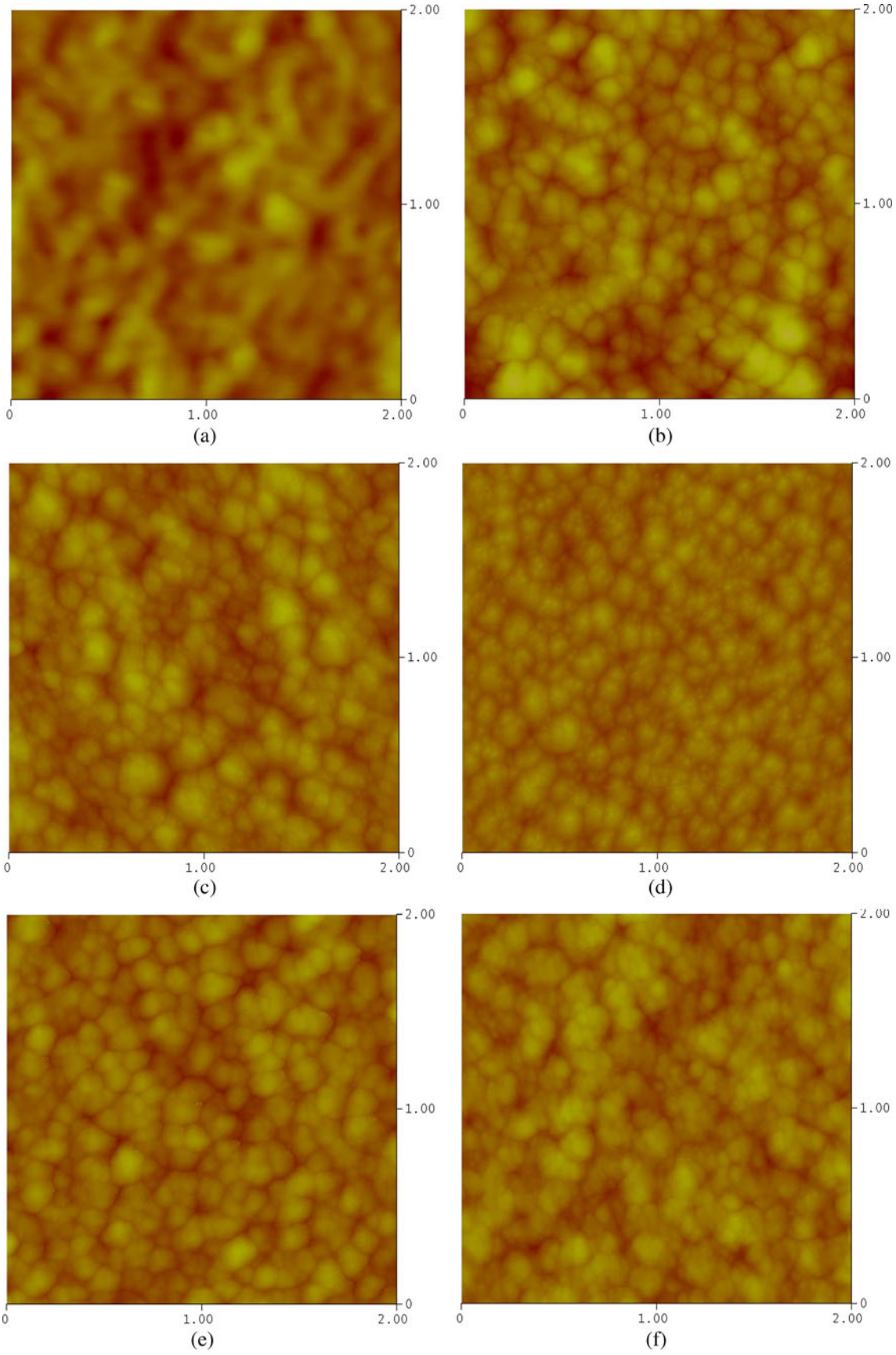

Figure 3. 2×2 μm two-dimensional AFM images of (**a**) pristine film and films irradiated with (**b**) 1×10^{11}, (**c**) 3×10^{11}, (**d**) 1×10^{12}, (**e**) 3×10^{12} and (**f**) 1×10^{13} ions cm^{-2}.

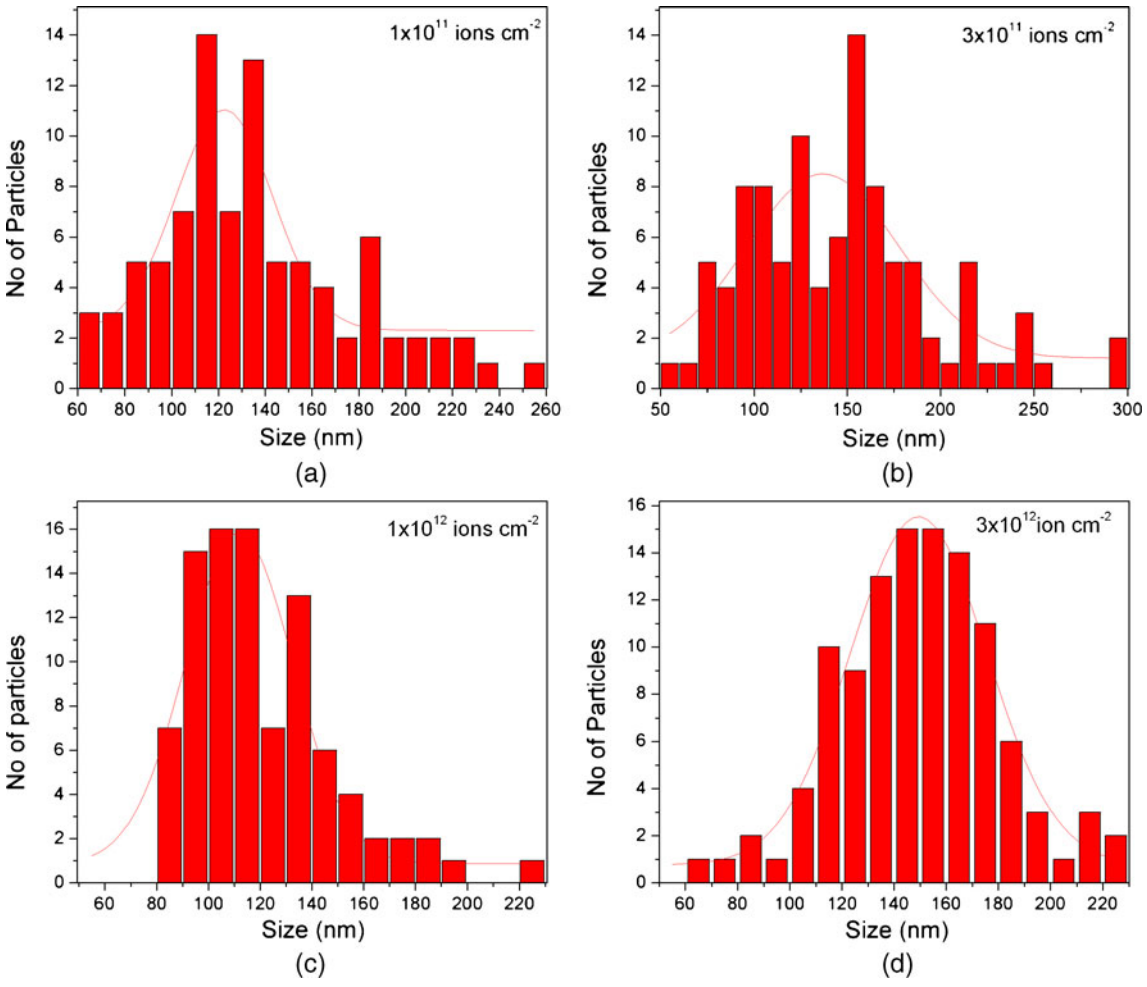

Figure 4. Size distribution of surface structures obtained from AFM images of films irradiated with (**a**) 1×10^{11}, (**b**) 3×10^{11}, (**c**) 1×10^{12} and (**d**) 3×10^{12} ions cm^{-2}.

Table 1. Variation of average grain size, σ_{rms} and δ with ion fluence.

Fluence (ions cm^{-2})	Average grain size (nm)	σ_{rms} (nm)	Power law exponent (δ)
0	–	6·2	2·59 ± 0·06
1×10^{11}	123	12·7	2·95 ± 0·03
3×10^{11}	137	11·4	2·79 ± 0·02
1×10^{12}	112	7·3	2·94 ± 0·03
3×10^{12}	150	8·1	2·90 ± 0·04
1×10^{13}	–	6·8	2·93 ± 0·03

correlated with roughness scaling exponent, α, by the relation $\alpha = \frac{\delta}{2} - 1$ (Eklund *et al* 1993). The estimated values of α for the pristine and irradiated samples are in the range from 0·30 to 0·48. These values lying between 0 and 1 indicate that the corrugation of the surface is self-affine, where surface has unequal scaling invariance in different directions (Krim *et al* 1993).

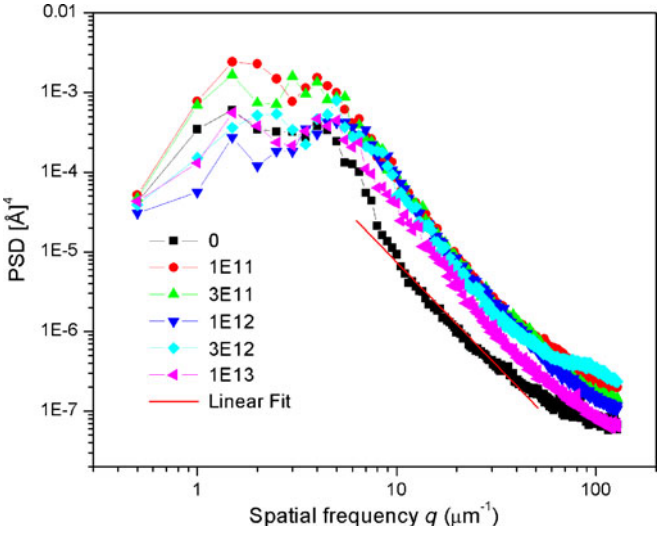

Figure 5. Variation of power spectral density (PSD) with spatial frequency, q, of surfaces for pristine as well as 200 MeV Ag ion irradiated $BiFeO_3$ films.

4. Conclusions

We report the evolution of surface morphology of $BiFeO_3$ thin films irradiated with 200 MeV Ag ions. We show that 200 MeV Ag ion irradiation led to reduced agglomeration of the grains with formation of sharper grain boundaries. The evolution of surface morphology of the pristine film is shown to be governed by the combined effect of evaporation–condensation and volume diffusion processes. SHI irradiation seems to increase the dominance of volume diffusion in controlling the surface morphology at different ion fluences.

Acknowledgements

The authors are thankful to Pelletron group of IUAC, New Delhi, for providing a good quality scanned beam for irradiation. Authors are also thankful to DST, Government of India, for providing AFM facility at IUAC, New Delhi, under IRPHA project. One of the authors (P D) would like to thank CSIR, New Delhi, Government of India, for the award of a SRF [Grant No. 09/173/(0127)/2010/EMR-I].

References

Agarwal D C, Chauhan R S, Avasthi D K, Khan S A, Kabiraj D and Sulania I 2008 *J. Appl. Phys.* **104** 024304

Bark C W, Cho K C, Koo Y M, Tamura N, Ryu S and Jang H M 2007 *Appl. Phys. Lett.* **90** 102904

Bea H, Gajek M, Bibes M and Barthelemy A 2008 *J. Phys. Condens. Matter* **20** 434231

Blaauw C and van der Woude F 1973 *J. Phys. C: Solid State Phys.* **6** 1422

Catalan G and Scott J F 2009 *Adv. Mater.* **21** 2463

Chen X, Hu G, Wu W, Yang C and Wang X 2010 *J. Am. Ceram. Soc.* **93** 948

Cheng L, Hu G, Jiang B, Yang C, Wu W and Fan S 2010 *Appl. Phys. Exp.* **3** 101501

Eklund E A, Snyder E J and Williams R S 1993 *Surf. Sci.* **285** 157

Fiebig M, Lottermoser Th, Fröhlich D, Golsev A V and Pisarev R V 2002 *Nature* **419** 819

Fujino S *et al* 2008 *Appl. Phys. Lett.* **92** 202904

Herring C 1950 *J. Appl. Phys.* **21** 301

Hill N A 2000 *J. Phys. Chem. B* **104** 6694

Iakovlev S, Solterbeck C H, Kuhnke M and Es-Souni M 2005 *J. Appl. Phys.* **97** 094901

Ihlefeld J F *et al* 2008 *Appl. Phys. Lett.* **92** 142908

Kartavtseva M S, Gorbenko O Yu, Kaul A R, Murzina T V, Savinov S A and Barthélémy A 2007 *Thin Solid Films* **515** 6416

Kim J K, Kim S S, Park M H, Choi E J, Kim J W, Guo R and Bhalla A S 2006 *Ferroelectrics* **345** 77

Krim J, Heyvart I, Haesendonck D V and Bruynseraede Y 1993 *Phys. Rev. Lett.* **70** 57

Kumaravel R, Ramamurthi K, Sulania I, Asokan K, Kanjilal D, Avasthi D K and Kulria P K 2011 *Radiat. Phys. Chem.* **80** 435

Kumar M, Ganesan P G, Singh V N, Mehta B R and Singh J P 2008 *Nanotechnology* **19** 175606

Lee S W and Kim C S 2006 *J. Magn. Magn. Mater.* **304** e772

Li Y, Yu J, Li J, Zheng C, Wu Y, Zhao Y, Wang M and Wang Y 2011 *J. Mater. Sci.* **22** 323

Li Y, Sritharan T, Zhang S, He X, Liu Y and Chen T 2008 *Appl. Phys. Lett.* **92** 132908

Li Y W, Sun J L, Chen J, Meng X J and Chu J H 2005 *J. Cryst. Growth* **285** 595

Liu H, Liu Z, Liu Q and Yao K 2006 *Thin Solid Films* **500** 105

Mallick P *et al* 2009 *Appl. Surf. Sci.* **256** 521

Mallick P, Biswal R, Rath C, Agarwal D C, Avasthi D K, Kanjilal D, Satyam P V and Mishra N C 2010 *Nucl. Instrum. Meth. Phys. Res.* **B268** 470

Mallick P, Agarwal D C, Rath C, Behera D, Avasthi D K, Kanjilal D and Mishra N C 2012 *Radiat. Phys. Chem.* **81** 647 (and references therein)

Michel C, Moreau J M, Achenbach G D, Gerson R and James W J 1969 *Solid State Commun.* **7** 701

Naganuma H and Okamura S 2007 *J. Appl. Phys.* **101** 09M103

Sahasrabudhe M S, Bankar D N, Banpurkar A G, Patil S I, Adhi K P and Kumar R 2007 *Nucl. Instrum. Meth. Phys. Res.* **B263** 407

Siwach P K, Singh H K, Singh J and Srivastava O N 2007 *Appl. Phys. Lett.* **91** 122503

Studer F, Hervieu M, Costantini J M and Toulemonde M 1997 *Nucl. Instrum. Meth. Phys. Res.* **B122** 449

Takahashi K, Kida N and Tonouchi M 2006 *Phys. Rev. Lett.* **96** 117402

Wang J *et al* 2004 *Appl. Phys. Lett.* **85** 13

Yang S Y *et al* 2005 *Appl. Phys. Lett.* **87** 102903